First-principles studies of the structural and optical properties of crystalline poly(*para*-phenylene)

C. Ambrosch-Draxl
Insitut für Theoretische Physik, Universität Graz, Austria

J. A. Majewski and P. Vogl
Physik Department and Walter Schottky Institut, Technische Universität München, Garching, Germany

G. Leising
Institut für Festkörperphysik, Technische Universität Graz, Austria
(Received 18 October 1994; revised manuscript received 2 December 1994)

We present first-principles local-density band structure calculations for one-dimensional and three-dimensional crystalline poly(*para*-phenylene) (PPP) using the full-potential linearized augmented-plane-wave and the pseudopotential methods. Optimized structural parameters for PPP chains and for orthorhombic crystalline phases with space groups *Pbam* and *Pnnm* are determined. A torsion angle of 27° is predicted in PPP chains and 17° in the crystals. The dielectric tensor and the absorption coefficient are calculated. We find very good agreement with experimental data, indicating that the excitations are extended band states. The interchain coupling leads to energy band splittings of the order of 0.5 eV. It is shown that the energy gap can be varied over a wide energy range by relatively small structural modifications.

I. INTRODUCTION

The recent fabrication of efficient light emitting diodes based on conducting polymers has been a breakthrough in the field of polymer electronics. Among the most promising materials for optical applications are crystalline poly(*para*-phenylene vinylene) (PPV) and poly(*para*-phenylene) (PPP). In particular, the pioneering work on electroluminescence from PPV (Ref. 1) and the discovery of blue light emission from PPP (Ref. 2) constitute exciting progress. However, the low stability and limited possibilities in tuning the wavelength of many conducting polymers as well as the difficulties in processing these materials that are often insoluble and infusible still hamper commercial applications. The wide-gap polymeric semiconductor PPP is stable in air up to 400 °C and several chemical methods have been developed that may provide means to successfully process and tailor its electronic and optical properties.[3–9]

In this work, we present first-principles studies of structural and optical properties of single-chain and crystalline, three-dimensional poly(*p*-phenylene) and compare it to experimental data. We investigate theoretically the influence of several structural modifications of PPP on the energy gap and the optical properties of PPP. The present calculations support the qualitative conclusions of Brédas[10] that the band gap of semiconducting polymers can be engineered in a wide range from red to ultraviolet by structural changes that may be realized by doping or the addition of side chains. We employ two different first-principles methods in this paper, namely, the full-potential linearized augmented-plane-wave (LAPW) method as well as the pseudopotential method. A detailed comparison between the two methods allows a critical assessment of their accuracy.

The precise atomic configuration in PPP is known only for finite oligomers but not for one-dimensional (1D) or three-dimensional (3D) crystalline phases of PPP. Therefore, a first-principles study of these materials must provide both structural parameters through total energy minimizations as well as optical properties for the optimized structures. Such calculations have been performed in the framework of the local-density-functional approach (LDA) primarily for 1D and 3D polyacetylene.[11–14] More recently, the band structure of 3D PPV was predicted by a LDA calculation employing the pseudopotential method.[15] This study showed that there is a very large interchain coupling that destabilizes polarons, analogously to what has been found before in 3D polyacetylene.[13] Systematic structural optimizations and energy gaps within LDA molecular dynamics calculations of several 1D polyenes have been reported by Brocks *et al.*[16] Brédas[10,17,18] have predicted the optimized structure and the band structure of PPP oligomers by Hartree-Fock calculations and by semiempirical studies.

In Sec. II, we discuss the available experimental data on the structure of PPP. An overview of the theoretical methods used in this paper is presented in Sec. III where we also summarize the computational details. The predicted optimized structure of PPP is presented in Sec. IV A, including the torsion angle between two adjacent phenyl rings determined for 3D and 1D PPP. The band structures of the crystalline forms of PPP with *Pbam* and *Pnnm* symmetry are discussed in Sec. IV B, with emphasis on the significant interchain interaction. In Sec. IV C, the predicted and measured dielectric func-

tion and absorption coefficient are compared to each other. Finally, Sec. IV D is devoted to the problem of tailoring the band gap and the optical properties of PPP by suitable variations of structural parameters.

II. CRYSTAL STRUCTURE OF PPP

Polyphenyls are formed by chains of phenyl rings (Fig. 1). The structures of phenylene oligomers and crystalline PPP have been studied extensively, but the space group and the structural parameters of crystalline PPP are still controversial. There exists a high-temperature $P2_1/a$ phase which is a common structure for planar organic molecules. The planar configuration, however, seems to be only an average of structures containing twisted rings. At low temperature, polyphenyls undergo several phase transitions that lead to nonplanar configurations.[19] In addition, the crystal structure, setting angles, and torsion angles also depend on the chain length. In p-terphenyl, two adjacent rings in a molecule are tilted with respect to each other by a torsion angle of 22.7° between two rings.[20] In p-quaterphenyl, the torsion angle is about 20°.[21] In PPP with long chains, an orthorhombic structure has been proposed with two molecular chains per unit cell.[22] Recent diffraction experiments on crystalline PPP have been interpreted in terms of the monoclinic space group $P2_1/n$. The monoclinic distortion, however, seems to be small or equal to zero.[22,23]

Another open question concerns the relative position and orientation of the neighboring chains with respect to each other in crystalline PPP. We will assume an orthorhombic space group for 3D PPP with two chains per unit cell in this paper. In general, each chain contains

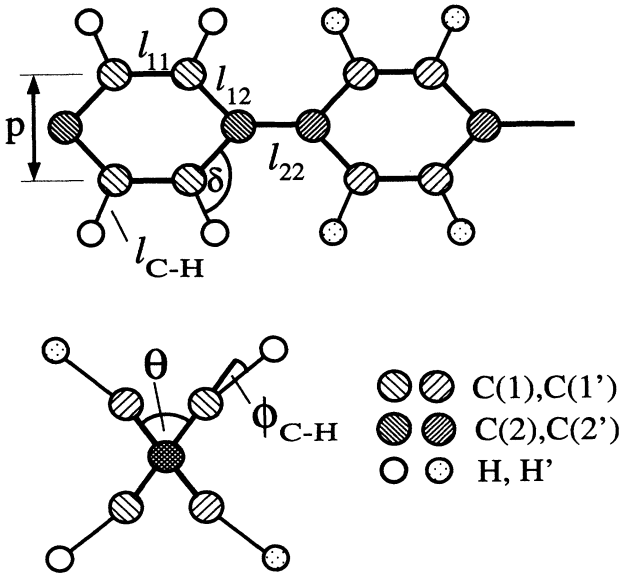

FIG. 1. Definition of structural parameters of PPP. The upper figure projects the repeat unit in a PPP chain onto a plane containing the chain axis, and the lower figure is a projection onto the plane perpendicular to the chain axis.

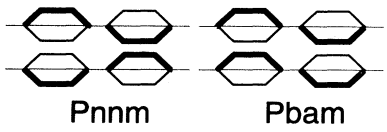

FIG. 2. Schematic projection of the unit cell of three-dimensional crystalline PPP with *Pnnm* symmetry (left) and *Pbam* symmetry (right) onto the a-c plane.

phenyl rings that are alternately twisted by some angle relative to each other. We therefore define the lattice constant c in the chain direction to contain two phenyl rings. For a finite twist angle, the two chains can either be shifted with respect to each other by an amount $c/2$ (space group *Pnnm*) or be unshifted (space group *Pbam*). These two possibilities are depicted in Fig. 2 and the atomic positions in the *Pbam* structure are shown in Fig. 3. Only for strictly planar chains with zero twist angle is a shift of $c/4$ also compatible with orthorhombic symmetry without a further doubling of the lattice parameter c.

In the present calculations, we optimize the atomic positions in the unit cell with first-principles methods. Only the lattice constants are taken from experiment,[24–26,23] namely, $a = 7.78$ Å, $b = 5.52$ Å, and $c = 8.54$ Å. a and b are measured average lattice constants with an error of about ±0.02, whereas the data show more scatter for the c parameter due to possible monoclinic distortions that depend on the conjugation length, degree of polymerization, and disorder.[27]

The following parameters characterize the geometry of the unit cell. The relative distances and angles between the atoms of one phenyl ring are denoted as l_{11}, l_{12}, $l_{C\text{-}H}$, p, δ, and $\phi_{C\text{-}H}$, respectively, and are depicted in Fig. 1. Since adjacent phenyl rings along the chain are generally not equivalent, the second ring may have different parameters, l'_{11}, l'_{12}, $l'_{C\text{-}H}$, p', δ', and $\phi'_{C\text{-}H}$. The bond connecting the two inequivalent rings along the chain has a length l_{22}. The torsion angle between these two rings is labeled as θ (see Fig. 1). In addition to these parameters, there is a setting angle ϕ_C that fixes the orientation of the plane of carbon atoms in one ring relative to the a-c plane. Correspondingly, the setting angles for the alternating phenyl rings in the same chain are $\phi_C + \theta$ and those of the rings on the neighboring chain in the

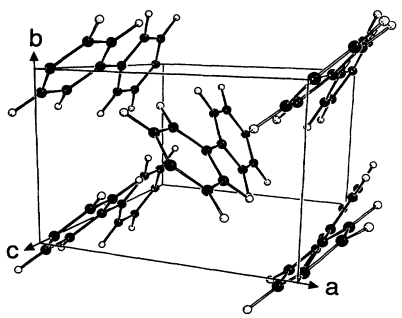

FIG. 3. Unit cell of three-dimensional crystalline PPP with *Pbam* structure.

orthorhombic unit cell are $180° - \phi_C$ and $180° - \phi_C - \theta$. Thus altogether there are 15 structural parameters for given lattice constants and space group that need to be optimized.

III. THEORETICAL METHODS

To calculate the ground state properties of PPP, we have employed the LAPW method as well as the *ab initio* pseudopotential plane-wave method in the framework of the LDA. Local-density-functional theory has been shown to accurately reproduce structural properties of a broad range of atoms, molecules, and solid-state systems, including polymers.[28] However, the LDA is also known to notoriously underestimate the energy gap of semiconducting systems. Fortunately, calculations of the electron self-energies have revealed that the true quasiparticle bands differ from the LDA bands for many materials predominantly by a rigid upward shift Δ_c of the conduction bands.[29] In fact, systematic LDA calculations for several polyenes have shown that one obtains, to a very good approximation, $E_{\rm gap}(\mathrm{LDA}) = 0.6\mathrm{E}_{\rm gap}(\mathrm{experiment})$.[16]

In the LDA approach, the total energy is expressed as

$$\begin{aligned} E_{\rm tot} &= E_{\rm tot,el} + E_{\rm core\text{-}core}, \\ E_{\rm tot,el} &= E_{\rm kin} + E_{\rm el\text{-}core} + E_{\rm el\text{-}el}, \end{aligned} \tag{3.1}$$

where $E_{\rm kin}$ is the kinetic energy of the electrons, $E_{\rm core\text{-}core}$ is the Coulomb interaction between the ion cores, $E_{\rm el\text{-}core}$ is the electron-core interaction, and $E_{\rm el\text{-}el}$ is the electron-electron interaction. The electronic energy $E_{\rm tot,el}$ is determined by solving self-consistently the Kohn-Sham equations[30,28]

$$\left[-\frac{\hbar^2}{2m}\nabla^2 + V_{\rm ion}(\mathbf{r}) + V_H(\mathbf{r}) + \mu_{\rm xc}(r)\right]\psi_i(r) = \epsilon_i\psi_i(r)\ . \tag{3.2}$$

Here, $V_{\rm ion}$ is the sum of the hydrogen and carbon ion core potentials, and V_H is the Hartree potential due to the valence charge density $\rho(\mathbf{r})$, and $\mu_{\rm xc}(\mathbf{r})$ is the exchange-correlation potential for electrons. $E_{\rm tot,el}$ can be obtained from

$$\begin{aligned} E_{\rm tot,el} = \sum_i^{\rm occ}\epsilon_i - \frac{1}{2}\int V_H(\mathbf{r})\rho(\mathbf{r})d\mathbf{r} \\ + \int[\epsilon_{\rm xc}(\mathbf{r}) - \mu_{\rm xc}(\mathbf{r})]\rho(r)dr\ , \end{aligned} \tag{3.3}$$

where $\epsilon_{\rm xc}(\mathbf{r})$ is the exchange-correlation energy density.

The cohesive energy is obtained by subtracting the total crystal energy $E_{\rm tot}$ from the total energy of the constituent, isolated atoms calculated with the local spin-density method.

Polymers possess many competing phases. Indeed, there are very small energy differences between a number of similar structures.[13,15] In order to obtain reliable solutions of the LDA equations that are not biased by approximations in the ionic potential, we have employed two different first-principles methods. The full-potential LAPW method provides the most faithful solution of the LDA equations Eq. (3.2) but it is difficult to optimize atomic positions in this method. Pseudopotential calculations, on the other hand, rely on a rigid-core approximation, but allow a straightforward computation of the Hellmann-Feynman forces.[31] We have therefore optimized the atomic positions with the pseudopotential method and then used the LAPW method for predicting the electronic and optical properties of PPP. In order to be able to estimate the reliability of both parameter-free methods, the total energy of 1D PPP and the band structure of 3D PPP at selected **k** points have been calculated within both methods.

The calculations for one-dimensional PPP chains have been carried out by embedding the chain in a three-dimensional supercell. By using orthorhombic unit cells with large lateral lattice constants $a = b = 7$ Å, we found interchain interactions to be negligible.

A. LAPW calculations

The full-potential linearized augmented-plane-wave (LAPW) calculations have been carried out using the optimized version WIEN93 of the originally published WIEN code.[32,33] We refer to this work for a detailed description of the method and only note the following computational details. The sphere radii of carbon and hydrogen have been chosen as 1.3 a.u. and 0.78 a.u., respectively. Within these spheres, the charge density and potential are expanded in terms of crystal harmonics up to angular momenta $L = 4$, and a plane-wave expansion with 2400 to 2800 Fourier coefficients has been used in the interstitial region.

Since the unit cells are very large in the present case, the Brillouin-zone integration can be performed by using only a few special **k** points.[34] The Brillouin-zone integrations for the total energy have been carried out using two special **k** points for three-dimensional PPP and six **k** points for one-dimensional PPP chains. The band structure and momentum matrix elements in the dielectric function, however, have been calculated on a grid of 704 special **k** points.

B. Pseudopotential calculations

The structural optimization of 1D and 3D PPP has been carried out by simultaneously relaxing all atomic positions in the unit cell until all first-order total energy derivatives with respect to the atomic positions vanish, i.e., by invoking the Hellmann-Feynman theorem. As discussed above, we have computed these forces within the pseudopotential method.[31] A separable, norm-conserving carbon pseudopotential was generated using the methods of Troullier and Martins[35] and Kleinman and Bylander.[36] We have tested the accuracy and transferability of this potential by applying it to bulk diamond and obtained the lattice constant, bulk modulus, and its pressure derivative, as well as the cohesive energy in excellent agreement with previous LDA calculations.[37] The

same pseudopotential has previously been used for C_{60}.[38] The Kohn-Sham equations Eq. (3.2) have been solved self-consistently with a preconditioned conjugate gradient algorithm.[39] The exchange-correlation functional was parametrized according to Ref. 40.

To ensure the numerical convergence of the calculated properties, we have used a cutoff kinetic energy of 60 Ry. In the case of a unit cell with 24 C and 16 H atoms, this implies the expansion of the wave function into 20 000 plane waves, leading to 160 000 Fourier components in the electronic density and the potential. In accord with previous results,[38] we have estimated the numerical error in the total energy $E_{\rm tot}$ to be less than 0.0125 eV/atom. The relatively slow convergence of the total energy in polymers is caused by the low-lying C σ energy bands. In cases where only the Bloch states near the Fermi energy matter, as is the case for the optical properties, it suffices to use much lower kinetic energy cutoffs of the order 25–30 Ry. Also, total energy differences between different crystal phases are converged to within 0.0001 eV/atom. In fact, they converge much faster than the total energy itself as is well known. Finally, we note that the residual forces on the atoms were smaller than 0.004 eV/Å. We estimate that the remaining relative error in all structural parameters is less than 1 %.

The difference in $E_{\rm tot}$ of 3D PPP by using one or four special **k** points[34] in the irreducible wedge (this is 1/8 of the Brillouin zone) is only 0.0025 eV/atom. All total energy calculations were therefore eventually carried out with one special **k** point and a 60 and 38 Ry cutoff energy for 3D PPP and 1D PPP, respectively.

C. Comparison between pseudopotential and LAPW calculations

We calculated the total energy of a single chain of PPP with alternately tilted phenyl rings as a function of the torsion angle θ, within the LAPW as well as within the pseudopotential method. The resulting total energy curves are depicted in Fig. 4. Both methods yield a minimum in the total energy at the same torsion angle of 27.4°. The small differences in the total energy for some values of θ between the two calculations are probably caused by residual interchain interactions. Similar agreement between the two theoretical approaches is found for the 3D crystal of PPP. In addition, we have compared the calculated eigenvalues of Eq. (3.2) for 3D PPP at selected **k** vectors as shown in Fig. 5. The calculated band eigenvalues (relative to the Fermi energy) differ by approximately 1% in the two methods.

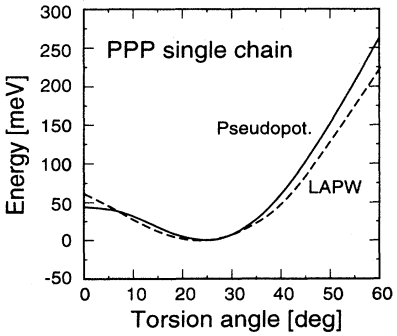

FIG. 4. Comparison between pseudopotential (full line) and LAPW (dashed line) calculations of the total energy (in meV) of one-dimensional PPP, as a function of the torsion angle θ (in degrees).

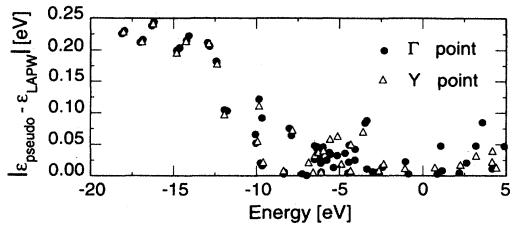

FIG. 5. Difference in band energies between pseudopotential and LAPW calculations in crystalline PPP for wave vectors $\mathbf{k} = (0,0,0) = \Gamma$ and $\mathbf{k} = (0, \pi/b, 0) = Y$ as a function of energy (in eV).

IV. RESULTS

A. Structural properties of PPP

We have optimized the geometry of a single infinite $(C_{12}H_8)_x$ chain as well as of the 3D crystalline phases with space groups *Pbam* and *Pnnm* of PPP. In Table I we summarize the predicted structural parameters, together with experimental data in oligomers.[21,23,41–43]

For both crystalline phases, *Pbam* and *Pnnm*, the calculated total energies as well as the structural parameters are identical within the computational errors. In addi-

TABLE I. Predicted and experimental structural parameters of PPP. The experimental data are from Refs. 21, 23, and 41–43.

Parameter	Crystal		Single chain	Expt.
	Pbam	*Pnnm*	*Pccn*	
l_{11} (Å)	1.375	1.375	1.378	1.356–1.409
l_{12} (Å)	1.398	1.398	1.399	1.371–1.425
p (Å)	2.394	2.396	2.401	2.342–2.405
$l_{\rm C\text{-}H}$ (Å)	1.100	1.100	1.100	0.960–1.129
δ (deg)	120.5	120.4	119.4	116–128
ϕ_C (deg)	44.8	44.6		41.6–49.4
$\phi_{\rm C\text{-}H}$ (deg)	-2.0	-2.0	-2.0	
l'_{11} (Å)	1.375	1.374	1.378	
l'_{12} (Å)	1.399	1.399	1.399	
p'(Å)	2.397	2.395	2.401	
$l'_{\rm C\text{-}H}$ (Å)	1.100	1.100	1.100	
δ' (deg)	120.3	120.4	119.4	
ϕ'_C (deg)	62.1	61.8		61.6–69.4
$\phi'_{\rm C\text{-}H}$ (deg)	1.9	1.6	1.7	
l_{22} (Å)	1.450	1.450	1.456	1.469–1.505
θ_C (deg)	17.3	17.2	27.4	20–27

tion, the tilted phenyl rings along one chain have the same internal structure and only differ by their setting angle ϕ_C and ϕ'_C relative to the a-c plane (see Fig. 1). The predicted setting angles are 45° and 62°. This implies an average setting angle of 53.5°, in good agreement with the average experimental value of 55.5°.[21] In addition, the calculations predict that the rings are slightly buckled, i.e., the plane of the hydrogen atoms is tilted with respect to the plane of the carbons by an angle $\phi_{C\text{-}H} \approx 2°$ (see Fig. 1). Similar results have been obtained for other polymers.[13]

In order to identify the role of crystalline packing, we have also studied isolated chains of PPP with a lattice constant c equal to the value in the crystalline phase, optimizing all other structural parameters. As shown in Table I, the main difference between the optimized 3D and this 1D PPP structure is the torsion angle $\theta = 27.4°$ which is significantly smaller in the crystalline phase. Indeed, it is well known that intermolecular forces favor a less buckled structure in the 3D crystalline environment.[17,18,27] The experimental data[27] in oligomers give values between 20° and 30°, in very good agreement with the present theoretical results. The gain in total energy by twisting adjacent phenyl rings is found to be 0.022 eV/ring = 0.51 kcal/mol for the single chain (one ring contains the formula unit C_6H_4) and 0.0075 eV/ring = 0.17 kcal/mol in both 3D crystalline phases. The present LDA calculations predict a gain of 0.279 eV/ring (6.43 kcal/mol) in the cohesive energy by forming a crystalline phase relative to isolated chains. For comparison, we note that the difference in total energies between the three energetically lowest phases of crystalline carbon, namely, cubic diamond, hexagonal diamond, and the bc-8 structure, is 0.03 and 0.69 eV/atom, respectively.[44]

B. Band structures of three-dimensional PPP

Figures 6 and 7 show the LAPW band structures for both crystalline phases of PPP with space groups *Pbam* and *Pnnm*, respectively. The minimal energy gap is 3.0 eV in the latter structure and smaller by 0.085 eV in the former. These values already include a self-energy

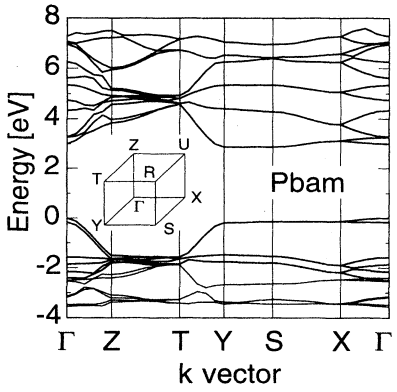

FIG. 6. Band structure of a 3D crystalline PPP with *Pbam* symmetry.

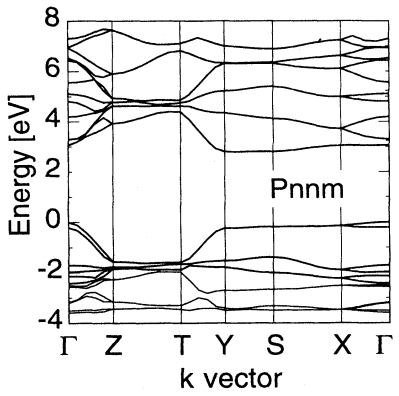

FIG. 7. Band structure of a 3D crystalline PPP with *Pnnm* symmetry.

$\Delta_c = 1.2$ eV for the conduction bands and agree very well with optical data, as will be discussed in more detail in Sec. IV C. A particularly noteworthy feature in these band structures is the large energy dispersion from the Brillouin-zone center Γ to the X point, which is of the order of 0.5 eV. Since this dispersion occurs *perpendicular* to the chain direction, this result indicates a substantial interaction across the chains. In fact, the same qualitative effect has been found previously in crystalline *trans*-$(CH)_x$,[13] and in crystalline PPV.[15] The physical origin of this interchain coupling is the electron-ion interaction between carbon atoms on neighboring chains mediated by hydrogen p states. The carbon π states that stick out of the C-H plane of one chain approximately point towards the closest hydrogen states of one of the neighboring chains. In Fig. 3, for example, the center C atoms of the middle chain interact with the closest H states of the upper left chain. Within one chain, the hydrogen s states do not couple to the C π states by symmetry. However, the hydrogen p states lie energetically close to the lowest unoccupied molecular orbital (LUMO) states in polymers and lead to the effective interchain C-C coupling that leads to the splitting of band states along the Γ-X axis as shown in Figs. 6 and 7.

There is a small but significant anisotropy in $\mathbf{k}_x$ and $\mathbf{k}_y$ that is related to the lattice constant a being larger than b. Indeed, the lowest conduction band state at $\mathbf{k} = Y$ has a lower energy than at X and Γ, whereas the highest valence band state occurs at the center of the Brillouin zone Γ. Thus the energy gap of crystalline PPP is slightly indirect and lower than the direct band gap by 0.24 eV in the *Pbam* structure and by 0.25 eV for *Pnnm*, respectively. In a perfect 3D crystal, this indirect band edge dramatically reduces the radiative emission efficiency since the emission process requires a phonon to guarantee momentum conservation. Since the energy gap in 1D PPP chains is direct and the available samples of 3D PPP are rather disordered, however, it is unlikely that this reduction in light emission plays a role in device applications.

C. Optical properties of three-dimensional PPP

We have computed the frequency-dependent complex dielectric tensor $\boldsymbol{\epsilon}(\omega)$ of crystalline PPP in the long-

wavelength limit, employing the self-consistent LAPW method. Since the space group is orthorhombic, the dielectric tensor is diagonal. We only show results for the *Pbam* structure here, since we found no significant difference for the *Pnnm* group. The imaginary part of the ith Cartesian component ($i = a, b, c$ for the directions along the crystal axes a, b, c) of the dielectric function is given by[45]

$$\text{Im } \varepsilon_i(\omega) = \frac{4\pi^2 e^2}{m^2(\omega - \Delta_c/\hbar)^2\, V} \sum_{v,c,\mathbf{k}} |\langle c\mathbf{k}|\mathbf{p}_i|v\mathbf{k}\rangle|^2 \times \delta(E_{c\mathbf{k}} - E_{v\mathbf{k}} - \hbar\omega), \quad (4.1)$$

where $\mathbf{p}$ is the momentum operator, and $E_{n\mathbf{k}}$ are the quasiparticle energies that we approximate by the LDA eigenvalues, shifted by the constant self-energy Δ_c for the conduction band states. The LDA Bloch functions are $|v\mathbf{k}\rangle$ and $|c\mathbf{k}\rangle$ for the valence and conduction bands, respectively. No damping is included in this equation in order to show the limiting case of $\boldsymbol{\varepsilon}$ in a perfect PPP crystal. We note that this expression takes into account the nonlocality of the self-energy operator and ensures gauge invariance.[45]

The real part of $\boldsymbol{\varepsilon}(\omega)$ has been obtained by the Kramers-Kronig relations. The interband absorption coefficient is given by

$$\alpha_i(\omega) = \sqrt{2}\,\frac{\omega}{c}\sqrt{|\varepsilon_i| - \text{Re}\varepsilon_i}. \quad (4.2)$$

Figure 8 shows all three Cartesian components of Im$\boldsymbol{\varepsilon}$. As is to be expected for a quasi-one-dimensional material, we find the anisotropy to be very pronounced. If one considers the ratio of Re$\varepsilon_c(0)$/Re$\varepsilon_a(0)$ as a measure for the average optical anisotropy, PPP is less anisotropic than *trans*-polyacetylene; this ratio equals 2.5 in PPP and 4.2 in *trans*-$(CH)_x$.[46] The maximum values of Imε_c and Imε_a differ by one order of magnitude in PPP. In PPV,[47] the ratio of these maximal values is approximately equal to that in PPP but it is significantly larger (≈ 50) in *trans*-$(CH)_x$.[46] Finally, we note that the component of Imε_c parallel to the chain axis shows the typical 1D-type singularity at the band edge.

Experimentally, the real and imaginary parts of the dielectric function have been determined up to an energy of 20 eV, employing high-energy electron loss spectroscopy (EELS).[48] For low momentum transfer (≤ 0.1 Å), these experimental data accurately reflect the dielectric function in the long-wavelength limit. In Fig. 9, the calculated Imε_c is shown as a function of energy and compared to these experimental data.[48] The overall agreement between theory and experiment is excellent, in spite of the fact that the present calculations neglect excitonic effects. It is interesting to note that it has recently been argued that excitonic binding energies in PPV are only of the order of k_BT.[49] However, optical data[50] in poly(phenylphenylenevinylene) as well as detailed calculations[51] in PPV suggest larger binding energies of the order of 0.4 eV. Since the present LDA calculations leave an uncertainty in the fundamental band gap of the order of a few tenths of an eV, excitons in PPP may well shift the onset of absorption by such an amount but do not seem to lead to other dominant effects in the optical spectrum.

Both the data and the calculations show essentially two peaks in Im$\boldsymbol{\varepsilon}$, namely, one near 3 eV and the second one near 6 eV. These transitions can easily be identified from the band structure depicted in Fig. 6. The bands in the Brillouin-zone plane $\Gamma \rightarrow X \rightarrow S \rightarrow Y \rightarrow \Gamma$ perpendicular to the chain direction show very little dispersion and give rise to a high joint density of states for highest occupied molecular orbital (HOMO) to LUMO transitions with energies of approximately 3 eV. The valence and conduction band states in the second plane $Z \rightarrow U \rightarrow R \rightarrow T \rightarrow Z$ perpendicular to the chain direction are separated by band gaps of about 6 eV and lead to the higher maximum in Im$\boldsymbol{\varepsilon}$.

The calculated interband absorption coefficient α_z is shown in Fig. 10 and compared to two different sets of experimental data.[52,53] Again, the agreement between theory and experiment is excellent, implying that the observed optical properties of PPP in the visible and uv frequency regime largely reflect intrinsic properties of the ordered material and are not sensitive to the disorder in the real samples.

D. Band gap engineering by structural modifications

The most intriguing application of PPP so far has been the successful fabrication of blue light emitting diodes (LED's).[2] LED's require an efficient carrier recombination across the energy gap and a sufficiently high mobility

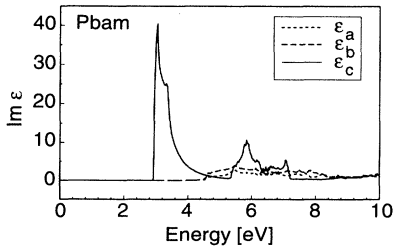

FIG. 8. Calculated imaginary part of the long-wavelength dielectric tensor in crystalline PPP in the *Pbam* phase. Its components parallel to the crystal axes a, b, and c are denoted by $\varepsilon_a, \varepsilon_b$, and ε_c, respectively, and are shown as a function of energy (in eV).

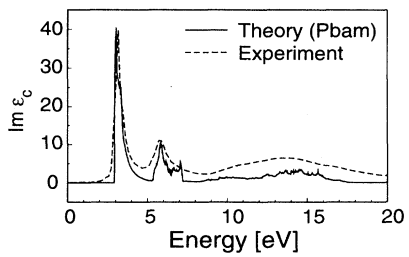

FIG. 9. Calculated component of the imaginary part of the dielectric function of crystalline PPP parallel to the chain axis, compared to the experimental data from Ref. 48.

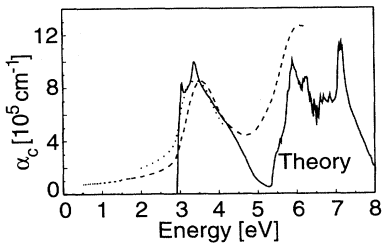

FIG. 10. Calculated c component of the absorption coefficient of crystalline PPP compared to the experimental data of Refs. 52 (dotted line) and 53 (dashed line).

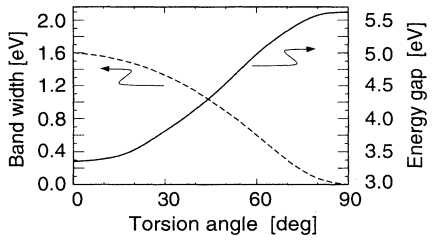

FIG. 12. Theoretical energy gap and bandwidth (in eV) of one-dimensional PPP as a function of the torsion angle θ.

of the carriers in order to be able to pump the emission process electrically. In highly oriented crystalline PPP, the carrier mobility along the chains is inversely proportional to the effective mass and therefore proportional to the band width. Thus, an optimization of PPP LED's with *ordered* structures must meet two criteria. First, the energy gap should lie in the blue frequency regime, and, second, the bandwidth of the lowest-lying conduction bands or topmost valence bands should be as large as possible.

We have studied theoretically the variation of the energy gap of the phenyl rings in PPP as a function of several structural modifications in order to provide guidelines for tailoring the band gaps and bandwidths to the requirements in device applications. Experimentally, these structural changes can only be achieved by introducing additional side chains or other methods of synthesis that are likely to alter many properties of PPP simultaneously. However, the present studies are hoped to provide some insight into how structural changes in the PPP chains affect the electronic and optical properties.

All calculations in this section have been carried out for single chains of PPP and the LAPW method has been employed throughout. As a starting point, we used the average experimental structure parameters of $l_{11} = 1.401$ Å, $l_{12} = 1.379$ Å, $l_{\text{C-H}} = 1.098$ Å, $p = 2.386$ Å, and $\delta = 126.1°$.[21,23,41–43] Figure 11 depicts the electronic band structure of such a chain with torsion angle θ set equal to zero.

Figure 12 shows the energy gap and the width of the topmost valence band as a function of the torsion angle θ between neighboring phenyl rings. In accord with a simple Hückel picture, the present first-principles calculations predict the energy gap to increase with increasing torsion angle. This originates in the inter-ring coupling between the C π orbitals which becomes weaker with increasing θ. Note that the limiting case of 90° gives a band gap that is similar to that of isolated benzene molecules. A difference remains, however, since the structural parameters differ from isolated benzene.

Next, we modify the distance l_{22} between rings and set the torsion angle θ equal to zero, leaving all other parameters unchanged (see Fig. 1). This modification implies a change in the chain lattice constant. Figure 13 depicts the minimal energy gap as a function of the *ratio* l_{12}/l_{22}. The full curve in this figure corresponds to a sole change of l_{22}, keeping l_{12} constant.

An alternative possibility to control the ratio l_{12}/l_{22} is to move the atoms that are labeled C(2) in Fig. 1 relative to the other C and H atoms along the chain axis but keeping the lattice parameter d equal to 4.27 Å. When l_{22} increases, one increases the aromatic character and the minimal energy gap increases,[10,17] as shown in Fig. 13. Conversely, by increasing the quinoid character, i.e., decreasing l_{22}, we can decrease the energy gap. Again, the bandwidths are found to change in inversely proportion to the gap as in the previous case.

These results show that the energy gap depends, to a good approximation, universally on this ratio l_{12}/l_{22}. As we will show in some detail below, a linear combination of atomic orbitals (LCAO) model in the two-center approximation fulfills this universality exactly.

Finally, we have performed LAPW calculations where

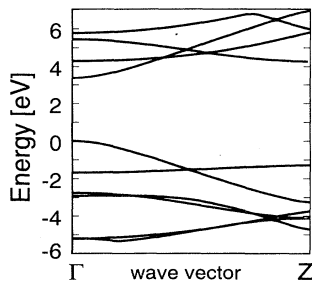

FIG. 11. Calculated band structure (in eV) of one-dimensional PPP for torsion angle $\theta = 0$ and lattice constant 4.27 Å.

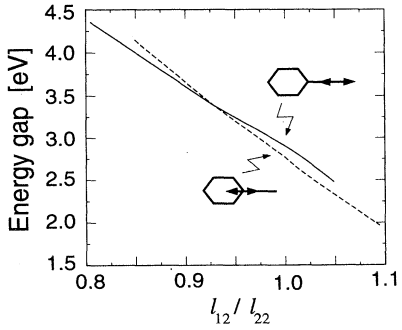

FIG. 13. Calculated energy gap of one-dimensional PPP (in eV) as a function of the ratio l_{12}/l_{22}. These structural parameters are defined in Fig. 1.

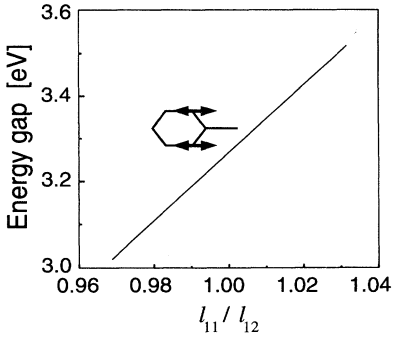

FIG. 14. Calculated energy gap of one-dimensional PPP (in eV) as a function of the ratio l_{11}/l_{12}.

the ratio l_{11}/l_{12} has been systematically varied. Again, the lattice constant $d = 4.27$ Å is kept constant. This structural modification is achieved by shifting the C atoms of type C(1) in Fig. 1 relative to the other types of atoms along the chain axis. The ideal aromatic ring corresponds to $l_{11}/l_{12} = 1$. It is plausible that one increases the quinoid character of the ground state and, correspondingly, decreases the energy gap by shortening the l_{11} bond. Indeed, the present first-principles calculations predict the energy gap to decrease linearly with the ratio l_{11}/l_{12}, as can be deduced from Fig. 14.

The results of these calculations can be condensed into a global picture of the energy gap by invoking a simple LCAO model for the infinite chain of PPP with one π orbital per carbon site. Corresponding to the distances l_{11}, l_{12}, and l_{22}, we allow for three different nearest-neighbor Hamiltonian matrix elements t_{ij}. It is convenient to measure all energies in units of t_{11} and set the diagonal Hamiltonian matrix element equal to zero. By forming six Bloch basis functions corresponding to the six states per unit cell, one can diagonalize the resulting 6×6 Hamiltonian matrix in the Bloch basis analytically and obtain, for each wave vector k, six band energies $\varepsilon_j(k)$, given by

$$\varepsilon_{1-4}(k) = \pm\left(2\alpha^2 + \frac{1+\gamma^2}{2} \pm \beta\right)^{1/2},$$
$$\beta^2 = \frac{1-\gamma^2}{2} + 4\alpha^2\left(\frac{1+\gamma^2}{2} + \gamma\cos ka\right),$$
$$\varepsilon_{5,6}(k) = \pm 1, \tag{4.3}$$

where $\alpha = t_{12}/t_{11}, \gamma = t_{22}/t_{11}$.

A special case of this equation was given in Ref. 18. The fundamental gap lies at $k = 0$. We now assume the tight-binding matrix elements to be universal functions of the bond lengths. Following Harrison's l^{-2} rule, we set $t_{ij} = \hbar^2\eta/(ml_{ij}^2)$, with $\eta = -0.81$.[54] The resulting energy gap is shown in Fig. 15 for a wide range of bond lengths. Even though this range is far greater than what can be realistically achieved experimentally, one can see that the topology of this energy surface is fairly smooth. Both

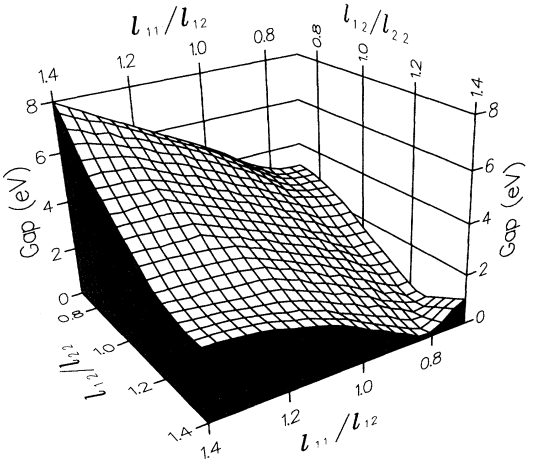

FIG. 15. LCAO model for the energy gap of one-dimensional PPP (in eV) as a function of the structural parameters l_{11}/l_{12} and l_{12}/l_{22}.

the absolute values and the trends in the energy gaps as a function of the structural parameters agree very well with the LDA results.

V. CONCLUSIONS

First-principles local-density calculations of structural and optical properties of one-dimensional and three-dimensional poly(*para*-phenylene) have been carried out. Excellent agreement is found with experimental data on the dielectric function and the absorption coefficient, indicating that neither disorder nor excitonic effects play a dominant role and that the electronic excitations can be represented by band states. The band structure of 3D PPP reveals that there is a significant interchain interaction that appears to be a universal feature of conjugated polymers. This interchain interaction renders the band edge states three-dimensional and consequently destabilizes the nonlinear excitations that are typical of one-dimensional systems.

We have shown that the band gap can be tuned through the whole visible region by fairly small structural changes that may be achieved by doping or adding suitable side chains. However, an increase of the band gap is always accompanied by a decrease in the bandwidth. Thus, a blue shift of the luminescence is accompanied by a decrease of the longitudinal dc conductivity in ordered PPP.

ACKNOWLEDGMENTS

This work was supported by the Jubiläumsfond der Österreichischen Nationalbank, Projekt No. 4420, and by the Volkswagenstiftung.

[1] J. H. Burroughes, D. D. C. Bradley, A. R. Brown, R. N. Marks, K. Mackay, R. H. Friend, P. L. Burns, and A. B. Holmes, Nature **347**, 539 (1990).
[2] G. Grem, G. Leditzky, B. Ullrich, and G. Leising, Adv. Mater. **4**, 36 (1992).
[3] L. W. Shacklette, H. Eckhardt, R. R. Chance, G. G. Miller, D. M. Ivory, and R. H. Baughman, J. Chem. Phys. **73**, 4098 (1980).
[4] D. L. Gin, V. P. Conticello, and R. H. Grubbs, J. Am. Chem. Soc. **114**, 3167 (1992).
[5] U. Scherf and K. Müllen, Makromol. Chem. **12**, 489 (1991).
[6] D. G. Ballard, A. Courtis, I. M. Shirley, and S. C. Taylor, Macromolecules **21**, 294 (1988).
[7] M. Rehan, A. D. Schlüter, and G. Wegner, Makromol. Chem. **191**, 1991 (1990).
[8] G. Leising, K. Pichler, and F. Stelzer, in *Electronic Properties of Conjugated Polymers III*, edited by H. Kuzmany, M. Mehring, and S. Roth (Springer, Heidelberg, 1989), p. 100.
[9] G. Grem and G. Leising, Synth. Met. **57**, 4105 (1993).
[10] J. L. Brédas, J. Chem. Phys. **82**, 3808 (1985).
[11] W. Mintmire and C. T. White, Phys. Rev. B **28**, 3283 (1983).
[12] J. Ashkenazi, W. E. Pickett, H. Krakauer, C. S. Wang, B. M. Klein, and S. R. Chubb, Phys. Rev. Lett. **62**, 2016 (1989).
[13] P. Vogl and D. K. Campbell, Phys. Rev. B **41**, 12 797 (1990).
[14] J. Paloheimo and J. von Boehm, Phys. Rev. B **48**, 16 948 (1993).
[15] P. Comes da Costa, R. G. Dandrea, and E. M. Conwell, Phys. Rev. B **47**, 1800 (1993).
[16] G. Brocks, P. J. Kelly, and R. Car, Synth. Met. **55-57**, 4243 (1993).
[17] J. L. Brédas, B. Thémans, J. G. Fripiat, J. M. André, and R. R. Chance, Phys. Rev. B **29**, 6761 (1984).
[18] J. M. André, J. Delhalle, and J. L. Brédas, *Quantum Chemistry Aided Design of Organic Polymers* (World Scientific, Singapore, 1991).
[19] J. L. Baudour, Acta Crystallogr. Sec. B **47**, 935 (1991).
[20] J. L. Baudour, Y. Delugeard, and P. Rivet, Acta Crystallogr. Sec. B **34**, 625 (1978).
[21] S. Sasaki, J. Polymer Sci. B **30**, 293 (1992).
[22] A. Kawaguchi and J. Petermann, Mol. Cryst. Liq. Cryst. **133**, 189 (1986).
[23] K. D. Aichholzer (unpublished).
[24] P. Kovacic, M. B. Feldman, J. P. Kovacic, and J. B. Lando, J. Appl. Polym. Sci. **12**, 1735 (1968).
[25] M. Stamm and J. Hocker, J. Phys. (Paris) Colloq. **44**, C3-667 (1983).
[26] M. Stamm, J. Fink, and B. Tieke, Mol. Cryst. Liq. Cryst. **118**, 281 (1985).
[27] K. N. Baker, A. V. Fratini, T. Resch, H. C. Knachel, W. W. Adams, E. P. Socci, and B. L. Farmer, Polymer **34**, 1571 (1993).
[28] For a review, see, e.g., R. O. Jones and O. Gunnarsson, Rev. Mod. Phys. **61**, 689 (1989).
[29] X. Zhu and S. G. Louie, Phys. Rev. B **43**, 14 142 (1991).
[30] W. Kohn and L. J. Sham, Phys. Rev. **140**, A1133 (1965).
[31] W. E. Pickett, Comput. Phys. Rep. **9**, 117 (1989).
[32] P. Blaha, K. Schwarz, P. Sorantin, and S. B. Trickey, Comput. Phys. Commun. **59**, 399 (1990).
[33] P. Blaha, K. Schwarz, and R. Augustyn (unpublished).
[34] H. J. Monkhorst and J. D. Pack, Phys. Rev. B **13**, 5188 (1976).
[35] N. Troullier and J. L. Martins, Phys. Rev. B **43**, 1993 (1991).
[36] L. Kleinman and D. M. Bylander, Phys. Rev. Lett. **48**, 1425 (1982).
[37] S. Fahy, K. J. Chang, S. G. Louie, and M. L. Cohen, Phys. Rev. B **35**, 5856 (1987); P. E. Van Camp, V. E. Van Doren, and J. T. Devreese, *ibid.* **38**, 12 675 (1988); A. Fukumoto, *ibid.* **42**, 7462 (1990).
[38] N. Troullier and J. L. Martins, Phys. Rev. B **46**, 1754 (1992).
[39] D. M. Bylander, L. Kleinman, and S. Lee, Phys. Rev. B **42**, 1394 (1990).
[40] J. P. Perdew and A. Zunger, Phys. Rev. B **23**, 5048 (1981).
[41] H. M. Rietveld, E. N. Maslen, and C. J. B. Clews, Acta Crystallogr. Sec. B **26**, 693 (1970).
[42] Y. Delugeard, J. Desuche, and J. L. Baudour, Acta Crystallogr. Sec. B **32**, 702 (1976).
[43] J. L. Baudour, H. Cailleau, and W. B. Yelon, Acta Crystallogr. Sec. B **33**, 1773 (1977).
[44] S. Fahy and S. G. Louie, Phys. Rev. B **36**, 3373 (1987).
[45] R. Del Sole and R. Girlanda, Phys. Rev. B **48**, 11 789 (1993).
[46] P. Vogl and G. Leising, Synth. Met. **41-43**, 3437 (1991).
[47] J. Fink, Adv. Electron. Electron Phys. **75**, 121 (1989).
[48] J. Fink, Synth. Met. **21**, 87 (1987).
[49] K. Pakbaz, C. H. Lee, A. J. Heeger, T. W. Hagler, and D. McBranch, Synth. Met. **64**, 295 (1994).
[50] R. Kersting, U. Lemmer, M. Deussen, H. J. Bakker, R. F. Mahrt, H. Kurz, V. I. Arhipov, H. Bässler, and E. O. Göbel, Phys. Rev. Lett. **73**, 1440 (1994).
[51] P. Gomes da Costa and E. M. Conwell, Phys. Rev. B **48**, 1993 (1993).
[52] B. Tieke, C. Bubek, and G. Lieser, Macromol. Chem. Rapid Commun. **3**, 261 (1982).
[53] G. Leising, H. Kreimaier, and R. H. Grubbs (unpublished).
[54] W. A. Harrison, *Electronic Structure and the Properties of Solids* (Freeman, San Francisco, 1980).